FEBS Letters 564 (2004) 294–300 FEBS 28179

# The plug domain of a neisserial TonB-dependent transporter retains structural integrity in the absence of its transmembrane β-barrel

M. Oke[a,b,c], R. Sarra[b], R. Ghirlando[a], S. Farnaud[c], A.R. Gorringe[d], R.W. Evans[c], S.K. Buchanan[a,b,*]

[a] *Laboratory of Molecular Biology, National Institute of Diabetes and Digestive and Kidney Diseases, National Institutes of Health, Department of Health and Human Services, Bethesda, MD 20892, USA*
[b] *Department of Crystallography, Birkbeck College, Malet Street, London WC1E 7HX, UK*
[c] *Metalloprotein Research Group, Division of Biomolecular Sciences, The Randall Centre for Molecular Mechanisms of Cell Function, King's College London, 3.6A New Hunt's House, Guy's Campus, London SE1 1UL, UK*
[d] *Research and Development, Health Protection Agency, Porton Down, Salisbury SP4 0JG, UK*

Received 15 December 2003; accepted 3 February 2004

First published online 28 February 2004

Edited by Fritz Winkler en Andreas Engel

**Abstract Transferrin binding protein A (TbpA) is a TonB-dependent outer membrane protein expressed by pathogenic bacteria for iron acquisition from human transferrin. The N-terminal 160 residues (plug domain) of TbpA were overexpressed in both the periplasm and cytoplasm of *Escherichia coli*. We found this domain to be soluble and monodisperse in solution, exhibiting secondary structure elements found in plug domains of structurally characterized TonB-dependent transporters. Although the TbpA plug domain is apparently correctly folded, we were not able to observe an interaction with human transferrin by isothermal titration calorimetry or nitrocellulose binding assays. These experiments suggest that the plug domain may fold independently of the β-barrel, but extracellular loops of the β-barrel are required for ligand binding.**


*Key words:* Transferrin binding protein A; Iron transport; Human transferrin; TonB; *Neisseria meningitidis*

## 1. Introduction

The Gram-negative genus *Neisseria* contains two pathogenic species, *N. gonorrhoeae* and *N. meningitidis*, the causative agents of gonorrhea and meningitis, respectively. Humans are the only hosts for these pathogens, possibly because *Neisseria* can only acquire iron efficiently from the human iron binding proteins hemoglobin, hemoglobin-haptoglobin [1–6], transferrin (hTf), and lactoferrin [1,7–12]. These host iron binding proteins have very high affinities for iron, thus reducing the level of free iron available for bacterial growth. Most bacteria synthesize and secrete low molecular weight siderophores, which also have high affinities for iron and are thus capable of competing for iron with host iron binding proteins [13]. Ferric siderophores are bound and transported into the periplasm by specific transporters in the outer membrane [14]. The transport mechanism appears to require proton motive force and a functional TonB-ExbB-ExbD complex, making it an active transport process [15]. In contrast to this mechanism of iron uptake, the pathogenic *Neisseria* species do not secrete siderophores [16–19] but express outer membrane proteins that bind and obtain iron directly from host iron proteins [20]. This process involves direct contact between the host iron protein and the outer membrane of the pathogen [17,18,21], as well as proton motive force and a neisserial TonB-ExbB-ExbD complex [22]. Iron uptake from hTf is mediated by the iron-repressible outer membrane complex, transferrin binding proteins A and B (TbpA and TbpB) [23]. TbpA (100 kDa) is an integral outer membrane protein and is well conserved among all strains of pathogenic *Neisseria* species [24]. TbpB is variable in size (68–85 kDa) and is a surface-exposed lipoprotein [25]. Each protein is capable of binding hTf independently, although the binding efficiency is increased in the presence of a TbpA-TbpB complex [26]. While TbpB is not required for iron uptake, TbpA serves as the channel for entry of iron into the cell and is therefore absolutely required [27].

TbpA has been proposed to fold similarly to FepA (ferric enterobactin transporter) and FhuA (ferric hydroxamate transporter), two *Escherichia coli* TonB-dependent siderophore transporters [28]. The crystal structures of FepA [29] and FhuA [30,31] show that each protein is composed of two domains: a 22-stranded β-barrel with large extracellular loops is embedded in the outer membrane, and an N-terminal globular domain is inserted into the barrel from the periplasmic side. Recently, the crystal structures of two additional *E. coli* TonB-dependent transporters, the ferric citrate transporter FecA [32,33] and the cobalamin transporter BtuB [34], were reported and are similar to the FepA and FhuA structures. Hence, it is anticipated that all TonB-dependent transporters will adopt the same basic two-domain architecture.

TonB-dependent transporters possess seven conserved regions [35], which have also been identified in TbpA [25,36]. One of these regions is referred to as the TonB box, a pentapeptide sequence located on the periplasmic side of the N-terminal domain (Fig. 1). The TonB box of the transporter is postulated to physically interact with TonB [37–41], resulting in transduction of energy from the inner membrane (derived

*Corresponding author. Fax: (1)-301-480 0597.
*E-mail address:* skbuchan@helix.nih.gov (S.K. Buchanan).

*Abbreviations:* TbpA, transferrin binding protein A; TbpB, transferrin binding protein B; hTf, human transferrin; HRP, horseradish peroxidase; PBS, phosphate-buffered saline; CD, circular dichroism; NRMSD, normalized root mean square deviation

0014-5793/04/$30.00 
doi:10.1016/S0014-5793(04)00196-6

from the proton gradient across the inner membrane) to the outer membrane transport proteins. TonB contains a single membrane-spanning α-helix, which anchors it in the inner membrane, and a large periplasmic domain, which interacts with the outer membrane transporter. The integral inner membrane proteins ExbB and ExbD interact with TonB, and are required for optimal energy transduction [42]. Consistent with other TonB-dependent transporters, gonococcal TbpA has also been demonstrated to interact with TonB [22]. Mutations in the TonB box of TbpA abolish iron transport, although TbpA is still able to bind hTf [43]. This demonstrates that TonB is required for transport of iron from hTf across the outer membrane.

The N-terminal domain of TonB-dependent transporters consists of a central four-stranded β-sheet, with several α-helices, β-strands and loops making up the rest of the structure (Fig. 1). It contains two (FepA), three (FhuA, FecA), or four (BtuB) loops that are positioned above the extracellular side of the lipid bilayer; residues from these loops form the floor of the binding pocket for the recognized ligand. The majority of the binding pocket is composed of residues from the extracellular loops of the barrel. The N-terminal domain completely blocks the β-barrel, making over 60 hydrogen bonds and numerous (nine or more) salt bridges with the β-barrel and extracellular loops. For this reason, it has been referred to as the plug [31], cork [30] or hatch [29] domain. Binding of ligand causes conformational changes in the plug domain, beginning with small changes at the extracellular side of the transporter that are propagated across the plug domain, with larger changes observed for residues at the periplasmic side of the transporter. The structures of FhuA and FecA in complex with their respective ligands reveal that a short α-helix, referred to as the switch helix (which is immediately preceded by the TonB box), unwinds and becomes disordered, possibly extending into the periplasm. This movement is suggested to bring the TonB box into contact with TonB. A FhuA mutant, in which the plug domain was constrained within the barrel via a disulfide bond, was incapable of transporting FhuA substrates [44], confirming the importance of the plug domain for ligand transport. However, none of the crystal structures reveals how the ligand is eventually transported. Siderophores range in size from 400 to 1500 Da, with ferric enterobactin (700 Da) having a radius of about 10 Å. Somehow the transporter must change its conformation to create a channel of the appropriate size, allowing bound ligand to be transported. Current hypotheses suggest a conformational rearrangement of the plug while it remains within the barrel [30,45] or complete removal of the plug from the barrel [46]. Expression of the FepA plug domain in the absence of its β-barrel yielded a polypeptide that was predominantly unfolded, but bound its cognate ligand with an affinity reduced by only 100-fold [47]. These authors therefore suggested that the fold of the plug domain might be only marginally stable, allowing the plug domain to unfold during ligand transport, thus facilitating either of the two hypothesized mechanisms.

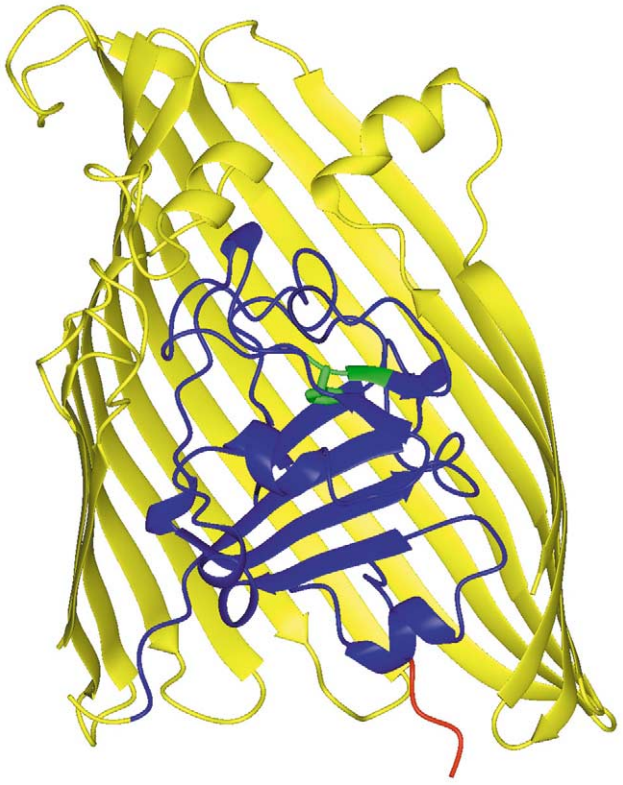

Fig. 1. Ribbon diagram of unliganded FecA prepared from the coordinates of the crystal structure [33]. The extracellular space is toward the top of the figure, and the periplasmic space is toward the bottom of the figure. The front β-strands of the barrel domain (yellow) have been removed to reveal the plug domain (blue) and the TonB box (red). The residues highlighted in green (F147 and G148) correspond to TbpA residues Y75 and S76. This figure was prepared with MOLMOL [65].

While the mechanism of ligand transport remains unknown, recent results from differential scanning calorimetry shed light on the folding behavior of the plug domain. Studies on FhuA suggest that the plug domain and the β-barrel behave as autonomous domains that unfold independently [48]. FhuA was observed to undergo two melting transitions at temperatures of 65°C and 75°C, corresponding to unfolding of the plug domain (plus portions of extracellular loops of the β-barrel) at the lower temperature, followed by unfolding of the β-barrel at the higher temperature. The first unfolding event was reversible, indicating that the plug domain may be able to fold (or refold) independently of the β-barrel.

To better understand the folding and ligand binding capabilities of a plug domain in the absence of its β-barrel, we have expressed the first 160 residues of TbpA from *N. meningitidis* (TbpA160) and characterized it by analytical ultracentrifugation, circular dichroism (CD) spectroscopy, and ligand binding analyses. Our results suggest that the plug domain has the expected secondary structure content when expressed in the cytoplasm or periplasm of *E. coli*, and the purified protein is monomeric and monodisperse in solution. TbpA160 does not bind hTf when analyzed by nitrocellulose binding assays or isothermal titration calorimetry, suggesting that the binding site for hTf is primarily composed of residues from the β-barrel domain.

## 2. Materials and methods

### 2.1. Cytoplasmic and periplasmic expression of the N-terminal domain of TbpA

The DNA encoding the N-terminal domain of TbpA (TbpA160) from *N. meningitidis* strain K454 (B:15:P1.7,16) was amplified by polymerase chain reaction (PCR) with Pfu polymerase (Stratagene) using the full-length *tbpA* gene as template. For cytoplasmic expres-

sion, the amplified fragment, encoding an N-terminal 10 histidine tag, was cloned into the expression vector pET17b (Novagen) using the *Nde*I and *Hin*dIII restriction sites. For periplasmic expression, a fragment was amplified by PCR corresponding to TbpA160, including an in-frame 5′ *Eco*RV recognition site and codons for 10 histidine residues at the N-terminus. The fragment was cloned into the *Eco*RV and *Hin*dIII restriction sites of pET20b (Novagen), which contains a *pelB* signal sequence and allows for periplasmic expression of TbpA160. *E. coli* BL21(DE3) (Novagen) competent cells were transformed with the resultant vectors.

### 2.2. Expression and purification of TbpA160 targeted to the cytoplasm or periplasm

For cytoplasmic expression of TbpA160, recombinant bacteria were grown in 2 l Luria broth, supplemented with carbenicillin (final concentration 100 μg/ml) at 30°C or 37°C under non-inducing conditions, to $OD_{600} = 3$–4. For periplasmic expression, recombinant bacteria were grown in 9 l of Terrific Broth (supplemented with carbenicillin as described above) at 20°C under non-inducing conditions, to $OD_{600} = 8$–10.

For both constructs, cells were harvested by centrifugation at 2500×*g*, 4°C for 30 min. Harvested cells (20 g) were resuspended in cold buffer containing 20 mM Tris–HCl, pH 8.0, 200 mM NaCl, and 0.4 mM AEBSF, and thoroughly mixed with a Dounce homogenizer. Next, 10 mM $MgCl_2$ and 100 μg/ml DNase I were added and the cell suspension was stirred at 4°C for 30 min. The cells were disrupted at 4°C using a French pressure cell at 18 000 psi (two passes). The cell lysate was centrifuged for 1 h at 39 000×*g*, yielding insoluble (pellet) and soluble (supernatant) fractions. The pellet and supernatant were analyzed for recombinant protein expression by sodium dodecyl sulfate–polyacrylamide gel electrophoresis (SDS–PAGE) [49]. For periplasmic expression, the periplasmic fraction was isolated by osmotic shock as described in the pET System Manual (Novagen).

For TbpA160 expressed in either the cytoplasm or periplasm, the supernatant was applied to a 10 ml nickel-nitrilotriacetate affinity column (Ni-NTA; Qiagen) at 4°C or room temperature, equilibrated with 50 mM $NaP_i$, pH 8.0, 200 mM NaCl, 30 mM imidazole, 10% (v/v) glycerol. The bound protein was eluted using a step gradient at 250 mM imidazole. The resulting peak fractions were pooled and concentrated using a YM10 ultrafiltration membrane (Millipore) and applied to a Sephacryl S-100 16/60 column (Amersham Biosciences) at 4°C or room temperature, equilibrated with 20 mM Tris–HCl, pH 8.0, 200 mM NaCl, 1 mM EDTA, 0.02% (w/v) $NaN_3$. Eluted protein fractions were analyzed for purity by SDS–PAGE. Final protein concentrations were determined by relating absorbance readings at 280 nm to the calculated TbpA160 extinction coefficient of 5120 $M^{-1}$ $cm^{-1}$. When necessary, a protease inhibitor cocktail consisting of 100 mM AEBSF, 80 μM aprotinin, 5 mM bestatin, 1.5 mM E-64, 7.5 mM phosphoramidon and 1 mM pepstatin A (Sigma) was added to all buffers at a ratio of 1:1000 (v/v).

### 2.3. Mass spectroscopy

Mass spectra were collected on a Micromass Platform single-quadrupole mass spectrometer (Micromass, Whatman, Altrincham, UK). A 10 μl sample was injected and the delivery solvent (50% (v/v) acetonitrile/50% water) was pumped at 10 μl/min. Twelve 10 s scans in positive ion mode were accumulated for each sample. The source temperature was set at 323 K. Spectra were processed using the Masslynx software supplied by Micromass (version 3.4).

### 2.4. Mutagenesis experiments

Mass spectroscopic analysis indicated a single proteolytic cleavage site between residues Y75 and S76 of TbpA160. Four mutations were introduced to prevent proteolysis: TbpA160-ΔY75, TbpA160-ΔS76, TbpA160-ΔY75S76 and TbpA160-Y75F. Mutagenesis experiments were carried out with the QuikChange Site-Directed Mutagenesis Kit (Stratagene) using the pET17b vector bearing the TbpA160 coding sequence as a template. The TbpA160 mutants thus obtained were verified by DNA sequencing (MWG, High Point, NC, USA) and expressed, purified and analyzed as previously described.

### 2.5. Analytical ultracentrifugation

Sedimentation equilibrium experiments were conducted at 4°C on a Beckman Optima XL-A analytical ultracentrifuge. A sample of TbpA160 (wild-type) was dialyzed against 200 mM NaCl and 20 mM Tris–HCl, pH 7.2, and the absorbance was adjusted to $A_{280} = 0.85$. A 160 μl sample was loaded into the cuvette and analyzed at different rotor speeds, ranging from 16 000 to 20 000 rpm. Data were acquired as an average of four absorbance measurements at a nominal wavelength of 280 nm and a radial spacing of 0.001 cm. Equilibrium was achieved within 48 h. Data were analyzed in terms of a single ideal solute to obtain the buoyant molecular mass, $M_1(1-\nu_1\rho)$, using the Optima XL-A data analysis software (Beckman) running under Microcal Origin 3.78, by fitting data from each scan to:

$$A_r = A_{o,1}\exp[HM_1(1-\nu_1\rho)(r^2-r_o^2)] + E$$

where $A_{o,1}$ is the absorbance at a reference point $r_o$, $A_r$ is the absorbance at a given radial position $r$, $H$ represents $\omega^2/2RT$, $\omega$ the angular speed in $rad^{-1}$, $R$ is the gas constant, $T$ is the absolute temperature and $E$ is a small baseline correction. Residuals were calculated. A random distribution of the residuals around zero (±0.02) was obtained as a function of the radius. Values of $M_1$ were obtained from the buoyant molecular mass, $M_1(1-\nu_1\rho)$, using the density, $\rho$, obtained from standard tables and the partial specific volume, $\nu_1$, calculated based on the amino acid composition using the published consensus data [50].

### 2.6. CD spectroscopy

Protein samples (0.5 mg/ml) were dialyzed against 20 mM $NaP_i$, pH 7.0. CD spectra were recorded using an AVIV 60DS spectropolarimeter controlled by AVIV 60DS v4.1i software. The wavelength range scanned was 300–190 nm. Measurements were made at 25°C in a rectangular cuvette of 0.2 mm path length. The data were processed using the SUPER3 software package described by Wallace and Teeters [51]. Spectra were normalized to the mean residue ellipticity by applying the scale factor:

$$0.1\times \mathrm{MRW}/([\mathrm{mg/ml}]\times \mathrm{pl})$$

where pl is the cuvette pathlength in centimeters and MRW is the mean residue weight (molecular weight divided by number of residues). The spectrum reported in Fig. 4 is the average of four scans taken at 1 nm/s. Data were corrected for the baselines by subtracting the data from buffer. After data collection, the spectrum was deconvoluted and data were analyzed for estimation of secondary structure composition using the Yang reference data [52]. The normalized root mean square deviation (NRMSD) parameter was calculated to determine the agreement between the experimental data and the calculated secondary structure. NRMSD is defined as:

$$\sum[(\theta\mathrm{exp}-\theta\mathrm{cal})^2/(\theta\mathrm{exp})^2]^{1/2}$$

where θexp represents the experimental ellipticity and θcal is the ellipticity of the back-calculated spectrum for the derived structure [53]. For comparison with the secondary structure of the FepA plug domain, the number of residues making up each secondary structure element was determined and expressed as a percentage of the total number of residues in the plug domain.

### 2.7. Nitrocellulose-based transferrin binding assay

The nitrocellulose-based transferrin binding assay has been described previously [11]. Briefly, serial dilutions (1:10) of the samples were prepared in phosphate-buffered saline (PBS), pH 7.4. Five μl of each dilution was blotted onto a nitrocellulose membrane (Bio-Rad), and left to dry for about 15 min. The membrane was blocked in 25 ml PBS, pH 7.4, containing 1% (w/v) milk powder for 1 h, with gentle shaking. The membrane was then washed in 25 ml distilled water, followed by three 5 min washes in PBS, before being probed with 1 μg/ml horseradish peroxidase-conjugated hTf (hTf-HRP) for 1 h, with gentle shaking. Bound hTf-HRP was visualized by the addition of 4-chloronaphthol (5 μg/ml) and 0.05% (v/v) $H_2O_2$, in PBS. Full-length TbpA containing an N-terminal $His_{10}$ tag, prepared essentially as previously described [54], was used as a control.

### 2.8. Isothermal titration calorimetry

The titration of TbpA160 with apo- or holo-hTf was carried out on a VP-ITC Microcalorimeter (Microcal, Northampton, MA, USA). A description of this instrument, including software and data analysis, has been provided [55]. Both apo- and holo-hTf were obtained from Sigma and added to the buffer without further purification. The pro-

teins were dialyzed against a buffer containing 10 mM HEPES buffer pH 7.5, 25 mM $NaHCO_3$, and 200 mM NaCl. Protein samples and buffer were filtered using a 0.22 μm filter (Millipore). TbpA160 was loaded into the sample cell (volume = 1.4 ml) at concentrations of 5 μM and 10 μM. hTf was loaded into the injection syringe (250 μl) and titrated into the sample cell at concentrations of 50 and 75 μM, respectively. A typical titration series involved a single 1 μl injection, followed by 29 injections of 10 μl titrant. The first injection was made over a 2 s interval, and subsequent injections were made over 20 s intervals. The baseline was allowed to stabilize for 240 s prior to subsequent additions to permit adequate time for reaction and equilibration. All experiments were performed at 25°C and the cell was stirred continuously at 310 rpm. For control experiments, all parameters were identical except that TbpA160 was replaced with buffer in the sample cell. The mean of the enthalpies measured from injection of ligand into buffer was subtracted from raw titration data prior to curve fitting using ORIGIN software (Microcal).

## 3. Results

### 3.1. Expression of TbpA160 and TbpA160 mutants

Cytoplasmic expression of TbpA160 produced recombinant protein recoverable from the soluble fraction, with none found in the insoluble fraction (Fig. 2, lanes 1 and 2). Periplasmic expression of TbpA160 produced soluble protein localized to the periplasmic fraction, with none found in the insoluble fraction (data not shown). However, the yield of protein from cytoplasmic expression was significantly higher than that from periplasmic expression (15 mg cytoplasmic TbpA160 per liter of culture compared with 0.3 mg periplasmic TbpA160 per liter of culture) so most experiments were performed with TbpA160 expressed in the cytoplasm.

Following cell lysis, TbpA160 (expressed in the cytoplasm or periplasm) was found to be sensitive to proteolysis, with two partially degraded products accumulating over time (Fig. 2, lane 4). To address this problem, the growth temperature was reduced from 37°C to 30°C, a protease inhibitor cocktail and 10% (v/v) glycerol were added to all purification buffers, and all procedures, including purification, were carried out at 4°C. These modifications led to a delay in proteolysis (Fig. 2, lane 5), with degraded products beginning to accumulate after 48 h for protein stored at both 4°C and −20°C. The molecular weights of the degraded products were examined by mass spectroscopy (data not shown). Two predominant peaks of

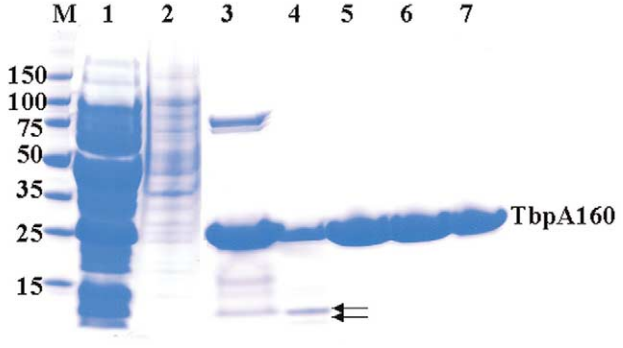


Fig. 2. Expression and purification of TbpA160. Samples of TbpA160 expressed in the cytoplasm were electrophoresed on 4–12% Bis-Tris gels (Invitrogen) using MES buffer. Lane M, molecular mass marker (15–150 kDa Perfect Protein Marker; Novagen); lane 1, soluble fraction; lane 2, insoluble fraction; lane 3, nickel column eluate; Lane 4, gel filtration column eluate; lane 5, TbpA160 after improved preparation (see text for details); lanes 6 and 7, TbpA160-ΔS76 and TbpA160-Y75F, respectively, after a 30 day incubation. Arrows indicate TbpA160 proteolytic fragments.

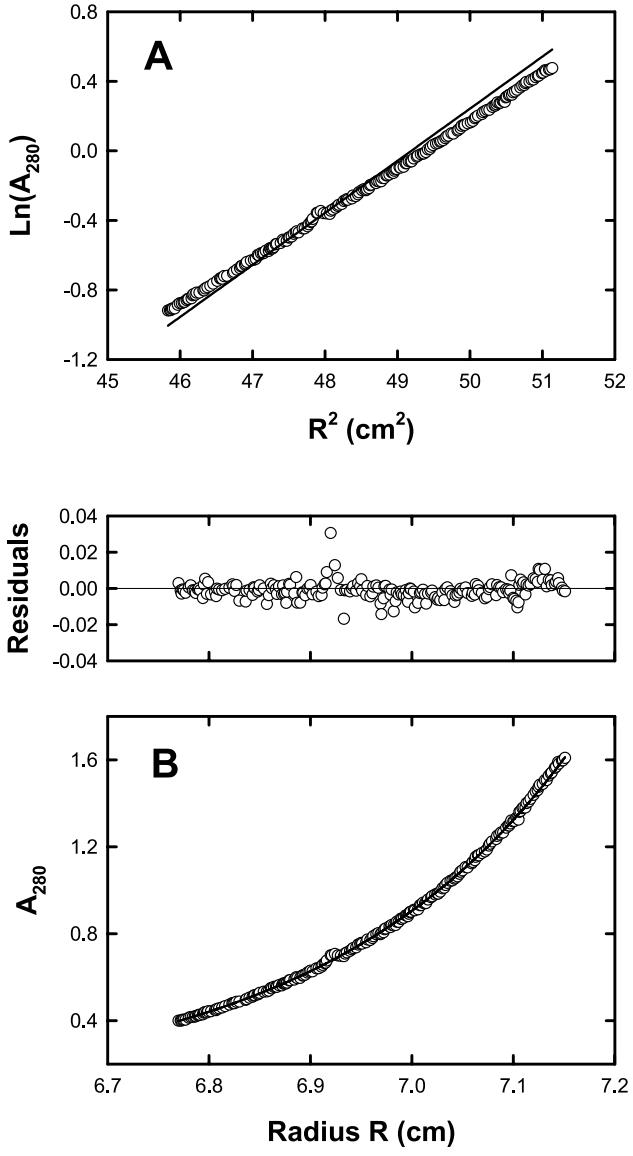


Fig. 3. TbpA160 is monodisperse and monomeric in solution. A: Sedimentation equilibrium profiles shown in terms of $\ln(A_{280})$ versus the square of the radius ($r^2$) for data collected at 16 000 rpm and 4°C. A linear plot corresponding to that expected for the TbpA160 monomer is shown to illustrate that the sample is monodisperse and monomeric. B: Sedimentation equilibrium profile at 16 000 rpm and 4°C shown as a distribution of $A_{280}$ at equilibrium. The results are analyzed for the best single component $M_1(1-\nu_1\rho)$ fit, shown as a line through the experimental points. The corresponding distribution of the residuals is shown above the plot.

9197.5 Da and 8296.25 Da were observed, which suggested a cleavage site between residues Y75 and S76. As an alternative approach to prevent proteolysis, three deletion mutations and one point mutation were separately introduced using site-directed mutagenesis. All four mutant proteins were expressed and purified as described for wild-type TbpA160. The TbpA160-Y75F and TbpA160-ΔS76 mutants displayed resistance to proteolysis, even after a 30 day incubation period at 4°C (Fig. 2, lanes 6 and 7), whereas the TbpA160-ΔY75 and TbpA160-ΔY75S76 mutants exhibited proteolysis identical to wild-type TbpA160 (results not shown). Unfortunately, all mutants had a tendency to aggregate and were largely unfolded as determined by CD spectroscopy (results not shown),

therefore further characterization of TbpA160 was carried out using the wild-type protein.

### 3.2. Analytical ultracentrifugation suggests that TbpA160 is monomeric and monodisperse

SDS–PAGE analysis (Fig. 2) and gel filtration chromatography (results not shown) showed that TbpA160 migrates as a 25 kDa protein, which is somewhat higher than the calculated value of about 18.3 kDa. We investigated the oligomerization state of wild-type Tbp160 by performing sedimentation equilibrium experiments. At all rotor speeds, data were best modeled in terms of a single ideal solute, determined as described in Section 2. The sample was found to be monodisperse, as identical values of $M_1(1-\nu_1\rho)$ were obtained at all rotor speeds (Fig. 3). An average value of $4640 \pm 120$ g/mol for $M_1(1-\nu_1\rho)$ was obtained, corresponding to a measured molecular mass of $17\,230 \pm 450$ g/mol. The value obtained is close to the calculated molecular mass of TbpA160, indicating that under these conditions the protein is monomeric ($M_{calc}$ = 18 248 g/mol, $n = 0.94 \pm 0.02$).

### 3.3. CD spectroscopy suggests that TbpA160 is a folded protein

The CD spectrum of wild-type TbpA160 (Fig. 4) is characteristic of a folded protein with identifiable secondary structural elements. It shows two negative bands at approximately 208 nm and 222 nm (the 208 nm band is more intense) and a positive band centered at approximately 190–195 nm. These features are representative of a protein containing both α-helices and β-strands [56]. Deconvolution of the CD spectrum indicates that TbpA160 consists of 21% α-helix, 26% β-sheet, 14% β-turn and 39% random coil, with an NRMSD value of 0.067. An NRMSD value $< 0.1$ is a strong indication that the calculated secondary structure actually reflects the secondary structure content of the measured protein [57]. The secondary structure content calculated for the FepA plug domain from the crystal structure [29] is 19% α-helix and 24% β-sheet, which suggests that both plug domains share a common fold. CD spectra for TbpA160 expressed in the periplasm yielded similar results, indicating that the plug domain is folded when it is expressed in either cellular compartment (results not shown).

### 3.4. TbpA160 does not show detectable binding of hTf

Although purified full-length TbpA binds both apo- and holo-hTf as demonstrated by nitrocellulose ligand binding assays using hTf-HRP [58], TbpA160 did not show detectable binding when analyzed by this method. The full-length TbpA used in our control experiments showed the expected binding behavior (results not shown).

Full-length TbpA has also been demonstrated to bind hTf by isothermal titration calorimetry [59]. In these experiments, purified TbpA bound either apo- or holo-hTf, with calculated dissociation constants of 68.9 nM or 3.7 nM for holo- and apo-hTf, respectively. In both cases, binding was driven by a large negative enthalpy change, suggesting the formation of hydrogen bonds, van der Waals forces, and/or electrostatic interactions, upon association of transporter and ligand. In contrast, our preparations of purified TbpA160 showed no measurable interaction with either apo- or holo-hTf, while the full-length TbpA we used as a control yielded the expected calorimetric titrations (results not shown).

## 4. Discussion

The plug domain of TbpA is similar in sequence to the plug domains from other structurally characterized TonB-dependent transporters, showing 29% identity and 44% similarity to the FepA plug domain [28]. Analysis of the FepA plug domain from the crystal structure [29] showed that it has characteristics of globular proteins: its surface is hydrophilic, and it is stabilized by a hydrophobic core formed from its central four-stranded β-sheet. Its structure suggests that such a plug domain might be stable when expressed in the absence of the transmembrane β-barrel. From the sequence similarity

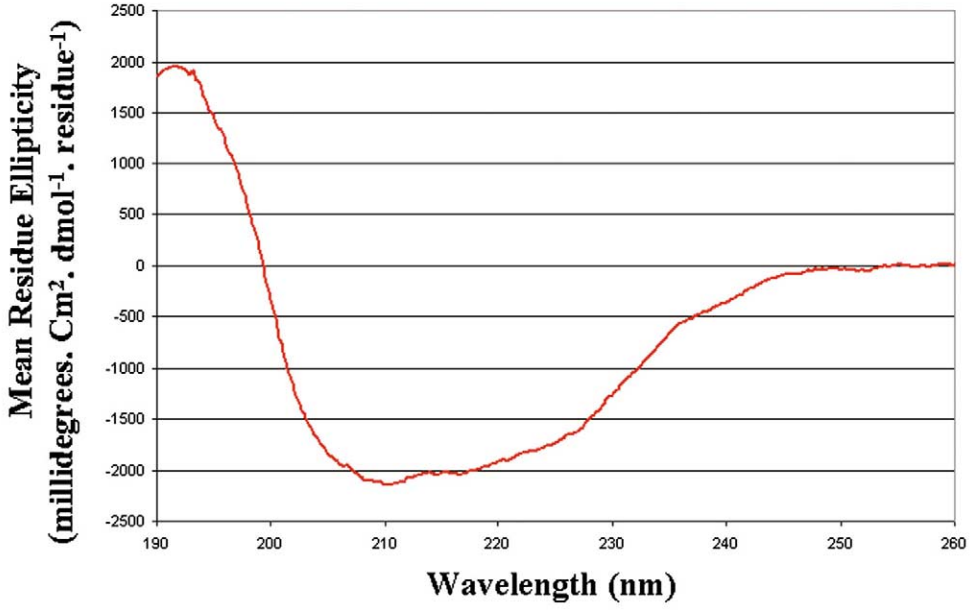


Fig. 4. CD spectrum of wild-type TbpA160 expressed in the cytoplasm. The spectrum shown is the average of four scans, and is representative of a folded protein, as described in Section 3. Conditions are as described in Section 2.

between the FepA and TbpA plug domains, we anticipate that the TbpA plug domain will adopt a similar structure.

The recovery of TbpA160 in the cytoplasmic or periplasmic fraction, in the absence of solubilizing agents such as detergents, suggests that this plug domain behaves as a soluble, globular protein that shows no association with the membrane. Soluble protein was also obtained for the expression of the predominantly unfolded FepA plug domain [47] and for a shorter TbpA plug domain construct which was not analyzed for secondary structure content [60]. The anomalous behavior of TbpA160 seen by size exclusion chromatography may reflect the elongated shape of the folded plug domain. Assessment by analytical ultracentrifugation showed that TbpA160 is monomeric and monodisperse under experimental conditions. Secondary structure analysis of TbpA160 by CD spectroscopy showed that TbpA160 contains very similar percentages of α-helix and β-strand to the FepA plug domain, as determined by X-ray crystallography [29]. Together these results suggest that TbpA160 adopts a native-like fold when expressed in the absence of its transmembrane β-barrel.

Proteolysis was observed in TbpA160 upon cell lysis, with a single proteolytic cleavage site found between residues Y75 and S76 by mass spectrometry. Residues Y75 and S76 are conserved in all TbpA sequences in pathogenic *Neisseria* species [25,36,61], *Actinobacillus pleuropneumoniae* (the causative agent of porcine pleuropneumonia), and *Haemophilus influenzae* (which is implicated in various diseases including meningitis and pneumonia) [36,61]. Although not conserved among all TonB-dependent transporters, these residues precede the IRG motif, which is conserved in these proteins. A structure-based sequence alignment of several TonB-dependent transporters shows that Y75 and S76 in TbpA correspond to F147 and G148 in FecA and to I72 and D73 in FepA, respectively [33]. Although the ligand binding site could not be determined for FepA [29], the FecA structure places the F147 and G148 residues in a loop involved in forming the floor of the binding pocket for citrate and ferric citrate (Fig. 1) [33]. Since no degradation is observed in full-length TbpA (M. Oke, R.W. Evans and S.K. Buchanan, unpublished results) it is likely that independent isolation of TbpA160 exposes site(s) that would otherwise be protected by the β-barrel domain. Nevertheless, the degradation process was delayed long enough to permit successful characterization of TbpA160. In a related experiment, the empty (plugless) barrel domain of FhuA showed an increased sensitivity to proteolysis and a decreased thermal stability, whereas wild-type FhuA (containing both plug and barrel) is protease-resistant [48]. These experiments suggest that the plug domain stabilizes and protects the β-barrel, and the barrel also protects the plug domain.

It was reported that the FepA plug domain is predominantly unfolded when expressed without its β-barrel [47]. Contrary to this, we found the homologous TbpA plug domain to be folded, with well-defined secondary structural elements similar to the plug domain of the FepA crystal structure. Previously, FepA and FhuA plugless proteins were reported to be capable of TonB-dependent ligand transport [46,62]. However, two groups have recently shown that the bacterial strains used in these studies, while having (partial) chromosomal deletions of the investigated transporters, retained chromosomal plug fragments (encoding the plug domain plus some residues of the β-barrel). The chromosomal plug fragments apparently complemented empty barrels expressed from a plasmid, resulting in functional transport of ferric ligands [63,64]. According to these authors, the TonB-dependent transport activity reported for plugless transporters was due to the subsequent addition of the plug domain by the host strain. If this is the case, it provides further evidence that the plug domain is capable of folding independently of the β-barrel, since it implies that an already folded plug domain can be incorporated into the separately expressed β-barrel.

The crystal structures of transporter–substrate complexes show that substrate binding involves a few residues in the loops of the plug domain and several more residues in the extracellular loops of the β-barrel [30–34]. The predominantly unfolded FepA plug domain, independent of the β-barrel, was reported to bind to ferric enterobactin, although with lower affinity relative to full-length FepA [47]. In contrast to the FepA plug results but in agreement with observations made for a shorter N-terminal TbpA construct [60] we did not observe any interaction between TbpA160 and hTf. Furthermore, hTf binding was completely abolished in TbpA mutants with deletions in several putative β-barrel loops [28], suggesting that the N-terminal domain of TbpA is not a significant contributor to ligand binding, but the extracellular loops of the barrel are very important. Since hTf is much larger than ferric siderophores (80 kDa versus 400–1500 Da), the binding site on TbpA may be more extensive, involving a greater number of residues and a larger binding surface, than what has been seen to date in siderophore transporters.

In conclusion, we have shown that the N-terminal domain of TbpA is soluble, monodisperse, and most likely correctly folded in solution, although incapable of binding hTf. Our results suggest that the two domains of TbpA, and other TonB-dependent transporters, may fold independently after translocation across the inner membrane, with subsequent insertion of the folded plug domain into the β-barrel.

*Acknowledgements:* We thank Travis Barnard, Reinhard Grisshammer, Alison Hickman, and Tara Kirby for critically reading the manuscript. M.O. was supported by the Engineering and Physical Sciences Research Council, UK, and by the NIDDK intramural program, NIH, USA; R.G. was supported by the NIDDK intramural program, NIH, USA; S.F. was supported by the Wellcome Trust, UK; A.R.G.'s work at the Health Protection Agency, Porton Down, was supported by the UK Department of Health; S.K.B. was supported by the Biotechnology and Biological Sciences Research Council, UK, and by the NIDDK intramural program, NIH, USA.

## References

[1] Mickelsen, P.A. and Sparling, P.F. (1981) Infect. Immun. 33, 555–564.
[2] Dyer, D.W., West, E.P. and Sparling, P.F. (1987) Infect. Immun. 55, 2171–2175.
[3] Lewis, L.A. and Dyer, D.W. (1995) J. Bacteriol. 177, 1299–1306.
[4] Lewis, L.A., Gray, E., Wang, Y.P., Roe, A. and Dyer, D.W. (1997) Mol. Microbiol. 23, 737–749.
[5] Lewis, L.A., Gipson, M., Hartman, K., Ownbey, T., Vaughn, J. and Dyer, D.W. (1999) Mol. Microbiol. 32, 977–989.
[6] Chen, C.J., Elkins, C. and Sparling, P.F. (1998) Infect. Immun. 66, 987–993.
[7] Mickelsen, P.A., Blackman, E. and Sparling, P.F. (1982) Infect. Immun. 35, 915–920.
[8] Lee, B.C. and Schryvers, A.B. (1988) Mol. Microbiol. 2, 827–829.
[9] Schryvers, A.B. and Lee, B.C. (1989) Can. J. Microbiol. 35, 409–415.
[10] Schryvers, A.B. and Morris, L.J. (1988) Infect. Immun. 56, 1144–1149.

[11] Schryvers, A.B. and Morris, L.J. (1988) Mol. Microbiol. 2, 281–288.
[12] Gray-Owen, S.D. and Schryvers, A.B. (1993) Microb. Pathog. 14, 389–398.
[13] Neilands, J.B. (1995) J. Biol. Chem. 270, 26723–26726.
[14] Neilands, J.B. (1981) Annu. Rev. Biochem. 50, 715–731.
[15] Moeck, G.S. and Coulton, J.W. (1998) Mol. Microbiol. 28, 675–681.
[16] Norrod, P. and Williams, R.P. (1978) Infect. Immun. 21, 918–924.
[17] Archibald, F.S. and DeVoe, I.W. (1979) FEMS Microbiol. Lett. 6, 159–162.
[18] Simonson, C., Brener, D. and DeVoe, I.W. (1982) Infect. Immun. 36, 107–113.
[19] West, S.E. and Sparling, P.F. (1985) Infect. Immun. 47, 388–394.
[20] Schryvers, A.B. and Stojiljkovic, I. (1999) Mol. Microbiol. 32, 1117–1123.
[21] McKenna, W.R., Mickelsen, P.A., Sparling, P.F. and Dyer, D.W. (1988) Infect. Immun. 56, 785–791.
[22] Kenney, C.D. and Cornelissen, C.N. (2002) J. Bacteriol. 184, 2027–2033.
[23] Gray-Owen, S.D. and Schryvers, A.B. (1996) Trends Microbiol. 4, 185–191.
[24] Cornelissen, C.N., Anderson, J.E., Boulton, I.C. and Sparling, P.F. (2000) Infect. Immun. 68, 4725–4735.
[25] Legrain, M., Mazarin, V., Irwin, S.W., Bouchon, B., Quentin-Millet, M.J., Jacobs, E. and Schryvers, A.B. (1993) Gene 130, 73–80.
[26] Cornelissen, C.N. and Sparling, P.F. (1996) J. Bacteriol. 178, 1437–1444.
[27] Anderson, J.E., Sparling, P.F. and Cornelissen, C.N. (1994) J. Bacteriol. 176, 3162–3170.
[28] Boulton, I.C., Yost, M.K., Anderson, J.E. and Cornelissen, C.N. (2000) Infect. Immun. 68, 6988–6996.
[29] Buchanan, S.K. et al. (1999) Nat. Struct. Biol. 6, 56–63.
[30] Ferguson, A.D., Hofmann, E., Coulton, J.W., Diederichs, K. and Welte, W. (1998) Science 282, 2215–2220.
[31] Locher, K.P., Rees, B., Koebnik, R., Mitschler, A., Moulinier, L., Rosenbusch, J.P. and Moras, D. (1998) Cell 95, 771–778.
[32] Ferguson, A.D., Chakraborty, R., Smith, B.S., Esser, L., van der Helm, D. and Deisenhofer, J. (2002) Science 295, 1715–1719.
[33] Yue, W.W., Grizot, S. and Buchanan, S.K. (2003) J. Mol. Biol. 332, 353–368.
[34] Chimento, D.P., Mohanty, A.K., Kadner, R.J. and Wiener, M.C. (2003) Nat. Struct. Biol. 10, 394–401.
[35] Kadner, R.J. (1990) Mol. Microbiol. 4, 2027–2033.
[36] Cornelissen, C.N., Biswas, G.D., Tsai, J., Paruchuri, D.K., Thompson, S.A. and Sparling, P.F. (1992) J. Bacteriol. 174, 5788–5797.
[37] Heller, K.J., Kadner, R.J. and Gunther, K. (1988) Gene 64, 147–153.
[38] Schoffler, H. and Braun, V. (1989) Mol. Gen. Genet. 217, 378–383.
[39] Bell, P.E., Nau, C.D., Brown, J.T., Konisky, J. and Kadner, R.J. (1990) J. Bacteriol. 172, 3826–3829.
[40] Skare, J.T., Ahmer, B.M., Seachord, C.L., Darveau, R.P. and Postle, K. (1993) J. Biol. Chem. 268, 16302–16308.
[41] Cadieux, N., Phan, P.G., Cafiso, D.S. and Kadner, R.J. (2003) Proc. Natl. Acad. Sci. USA 100, 10688–10693.
[42] Higgs, P.I., Myers, P.S. and Postle, K. (1998) J. Bacteriol. 180, 6031–6038.
[43] Cornelissen, C.N., Anderson, J.E. and Sparling, P.F. (1997) Mol. Microbiol. 26, 25–35.
[44] Endriss, F., Braun, M., Killmann, H. and Braun, V. (2003) J. Bacteriol. 185, 4683–4692.
[45] Barnard, T.J., Watson Jr., M.E. and McIntosh, M.A. (2001) Mol. Microbiol. 41, 527–536.
[46] Scott, D.C., Cao, Z., Qi, Z., Bauler, M., Igo, J.D., Newton, S.M. and Klebba, P.E. (2001) J. Biol. Chem. 276, 13025–13033.
[47] Usher, K.C., Ozkan, E., Gardner, K.H. and Deisenhofer, J. (2001) Proc. Natl. Acad. Sci. USA 98, 10676–10681.
[48] Bonhivers, M., Desmadril, M., Moeck, G.S., Boulanger, P., Colomer-Pallas, A. and Letellier, L. (2001) Biochemistry 40, 2606–2613.
[49] Laemmli, U.K. (1970) Nature 227, 680–685.
[50] Perkins, S.J. (1986) Eur. J. Biochem. 157, 169–180.
[51] Wallace, B.A. and Teeters, C.L. (1987) Biochemistry 26, 65–70.
[52] Chang, C.T., Wu, C.S. and Yang, J.T. (1978) Anal. Biochem. 91, 13–31.
[53] Mao, D., Wachter, E. and Wallace, B.A. (1982) Biochemistry 21, 4960–4968.
[54] Oakhill, J.S., Joannou, C.L., Buchanan, S.K., Gorringe, A.R. and Evans, R.W. (2002) Biochem. J. 364, 613–616.
[55] Wiseman, T., Williston, S., Brandts, J.F. and Lin, L.N. (1989) Anal. Biochem. 179, 131–137.
[56] Manavalan, P. and Johnson Jr., W.C. (1983) Nature 305, 831–832.
[57] Brahms, S. and Brahms, J. (1980) J. Mol. Biol. 138, 149–178.
[58] Boulton, I.C., Gorringe, A.R., Allison, N., Robinson, A., Gorinsky, B., Joannou, C.L. and Evans, R.W. (1998) Biochem. J. 334, 269–273.
[59] Krell, T. et al. (2003) J. Biol. Chem. 278, 14712–14722.
[60] Masri, H.P. and Cornelissen, C.N. (2002) Infect. Immun. 70, 732–740.
[61] Pajon, R., Chinea, G., Marrero, E., Gonzalez, D. and Guillen, G. (1997) Microb. Pathog. 23, 71–84.
[62] Braun, M., Killmann, H. and Braun, V. (1999) Mol. Microbiol. 33, 1037–1049.
[63] Vakharia, H.L. and Postle, K. (2002) J. Bacteriol. 184, 5508–5512.
[64] Braun, M., Endriss, F., Killmann, H. and Braun, V. (2003) J. Bacteriol. 185, 5508–5518.
[65] Koradi, R., Billeter, M. and Wüthrich, K. (1996) J. Mol. Graphics 14, 51–55.